



Fe₃O₄ magnetic nanoparticles in the layers of montmorillonite as a valuable heterogeneous nanocatalyst for the one-pot synthesis of indeno[1,2-*b*]indolone derivatives in aqueous media

Javad Safari¹ · Narges Hosseini Nasab¹

Received: 26 August 2018 / Accepted: 30 October 2018
© Springer Nature B.V. 2018

Abstract

In the present work, iron oxide nanoparticles (Fe₃O₄-NPs) were prepared using a chemical coprecipitation method. At room temperature, Fe₃O₄-NPs are put in inter-lamellar space and external surfaces of montmorillonite (MMT) as a supported solid. The MMT@Fe₃O₄ was characterized by X-ray diffraction (XRD), scanning electron microscopy (SEM), energy-dispersive X-ray spectroscopy (EDX), vibrating sample magnetometer (VSM), thermogravimetric analysis (TGA) and Fourier transform infrared spectrophotometry (FT-IR). Then, indeno[1,2-*b*]indolone derivatives were catalyzed by magnetic MMT@Fe₃O₄-NPs. MMT@Fe₃O₄-NPs were found to be a recoverable organocatalyst for the effective synthesis of the indeno[1,2-*b*]indolone derivatives via one-pot multicomponent cyclocondensation of ninhydrin, 1,3-diketo compound and amine derivatives in water. The significant advantages of this method are excellent yield, mild conditions, eco-friendly catalyst, low expense, and not using an environmentally harmful catalyst or solvent.

Keywords MMT@Fe₃O₄ nanoparticles · Organocatalyst · Ninhydrin · Indeno[1,2-*b*]indolones · Multicomponent reactions

Introduction

A significant type of heterocyclic organic compounds is indeno[1,2-*b*]indoles. They have biological and pharmacological applications [1]. Recently, this class of compounds received considerable attention because they act as lipid peroxidation inhibitors [2], adenosine triphosphate/guanosine triphosphate-competitive inhibitors

✉ Javad Safari
safari@kashanu.ac.ir

¹ Department of Organic Chemistry, Faculty of Chemistry, University of Kashan, Kashan 87317-51167, Islamic Republic of Iran

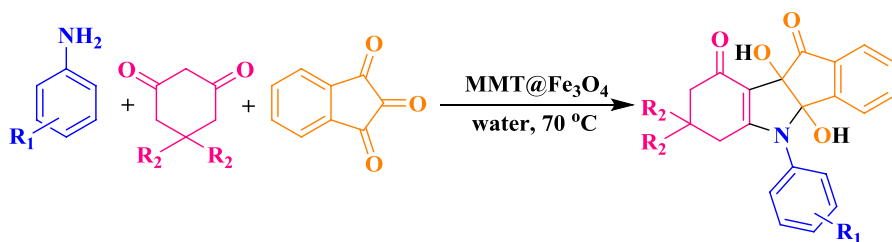
of protein kinase (CK2) [3], potassium channel openers [4], and estrogenic agents [5]. In some of the non-cancer illnesses (neurodegenerative disorders, inflammatory activities, angiogenesis illnesses, and viral infections) and cancer illnesses (such as prostate, colon, breast and lung cancers), indeno[1,2-*b*]indoles play a unique role [6, 7]. Because of these great features, we decided to explore the simple and effectual synthesis of indeno[1,2-*b*]indolone using MMT@Fe₃O₄ as a heterogeneous nanocatalyst under aqueous media.

In the last few years, remarkable regard has been paid to functional metal oxide nanocrystals such as Fe₃O₄ nanoparticles (Fe₃O₄-NPs) because of their prominent and technological applications as sensors, in clinical use, as catalysts and in high-density magnetic recording media [8]. Some other properties of Fe₃O₄-NPs include use as pigment, ferro fluids, in magnetic drug delivery, magnetic resonance imaging (MRI), data storage media, and recording material [9, 10].

Montmorillonite K10 (MMT-K10) as a catalyst and catalyst support is an example of the use of clays in chemical synthesis that has received special attention [11], due to their surface area in the range of 750 m²/g and high structural charge (up to 1000 meq/kg) [12]. MMT-K10 is a nanolayered aluminosilicate clay where one octahedral alumina sheet is sandwiched between two tetrahedral silica sheets, and can act as a nanoreactor for the chemical reactions and a drug nanocarrier for pharmaceutical targets. A large surface area, nonhazardous nature, non-corrosiveness, low cost, nano-sized, ease of handling, high stability and simple processing are the featured properties of MMT [13].

In particular, various methods for preparing magnetic NPs have been developed, including hydrothermal processes [14], the sol-gel method [15], the solvothermal method [16], and coprecipitation [17]. The simplest, most efficient and most economical method is coprecipitation.

In recent years, different methods have been introduced for the synthesis of dihydroxy indeno[1,2-*b*]indolone derivatives via multicomponent condensation of aromatic anilines, dimedone and ninhydrin as substrates with different catalysts such as SnO₂ quantum dots (QDs) [18] and C@TiO₂-SO₃H-IL1 [19]. However, these methods have their own merits, while use of an expensive catalyst, high reaction time, low product yield, and difficulties in a work-up procedure are their disadvantages. There are no examples of the use of MMT@Fe₃O₄ as a catalyst for the synthesis of dihydroxy indeno[1,2-*b*]indolone derivatives in aqueous media. Therefore, we report, for the first time, a new, efficient and clean methodology for the synthesis of dihydroxy indeno[1,2-*b*]indolone derivatives via three-component condensation of aromatic anilines, 1,3-diketo compounds, ninhydrin, and MMT@Fe₃O₄ as a heterogeneous catalyst in good yields and shorter reaction time in water (Scheme 1).



Scheme 1 Synthesis of dihydroxy indeno[1,2-*b*]indolone derivatives

Experimental section

Materials

All commercially available reagents were used without further purification and purchased from Merck and Sigma-Aldrich Company in high purity. The used solvents were purified by standard procedure.

Apparatus

Melting points were specified on an Electrothermal MK3 apparatus using an open-glass capillary and are uncorrected. Fourier transform infrared spectrophotometry (FT-IR) spectra were recorded as potassium bromide pellets with a Perkin-Elmer 550 spectrometer. Proton nuclear magnetic resonance (¹H NMR) and carbon-13 NMR (¹³C NMR) spectra were obtained in DMSO-d₆ solvent with a Bruker DRX-400 and Bruker Avance spectrometer at 400 and 100 MHz, respectively. Analytical thin-layer chromatography (TLC) was done on 0.2-mm precoated plates of silica gel 60 F-254 (Merck). The elemental analyses (C, H, N) were obtained from a Carlo ERBA Model EA 1108 analyzer. Nanostructures were specified using a Holland Philips Xpert X-ray powder diffraction (XRD) diffractometer (CuK α , radiation, $\lambda = 0.154056$ nm), at a scanning speed of 2°/min from 10° to 100° (2 θ). Scanning electron microscopy (SEM) analysis was performed on an MIRA3 from the TESCAN Company. Magnetic properties were determined by a vibrating sample magnetometer (VSM, MDKFD, University of Kashan, Kashan, Iran) at room temperature. Thermogravimetric analysis (TGA) was performed on a Mettler TA4000 system TG-50 at a heating rate of 10 K min⁻¹ under N₂ atmosphere. Energy-dispersive X-ray spectroscopy (EDX) was carried out using a LEVENS device equipped with an IDFix detector.

A procedure for MMT@Fe₃O₄ nanoclay

The MMT@Fe₃O₄ nanoclay was synthesized by chemical coprecipitation technique as described in the literature. The details are as follows: 1.0578 g of FeCl₂·4H₂O was dissolved in 100 mL of deionized water, 1.00 g of MMT was added to the mixture for 15 min, and the mixture was stirred for 30 min. Then, 2.5228 g of FeCl₃·6H₂O

was dissolved in the suspension by vigorously stirring the mixture solution for 30 min at 80 °C under N₂ atmosphere. Under the protection of nitrogen gas, 10 mL of NH₃·H₂O was added into the mixture rapidly, and the reaction mixture proceeded for another hour. Finally, the modified MMT@Fe₃O₄-NPs were magnetically separated and washed with distilled water and ethanol several times [20].

General procedure for the synthesis of indeno[1,2-*b*]indole-9,10-diones

A mixture of aromatic amine (1.0 mmol), 1,3-dicarbonyl compound (dimedone or 1,3-cyclohexadione; 1.0 mmol), and MMT@Fe₃O₄ (0.02 g) were stirred in 5 mL of water at 70 °C for 5 min. Afterward, ninhydrin (1.0 mmol) was added. After the completion of the reaction (monitored by TLC with hexane/AcOEt at a ratio of 1:2), the reaction was allowed to cool and the magnetic catalyst was removed by an external magnet. The precipitate was collected by filtration and washed with water multiple times. All of the products were identified by physical and spectroscopic data as follows;

*4b,9b-Dihydroxy-7,7-dimethyl-5-phenyl-4b,5,7,8-tetrahydroindeno[1,2-*b*]indole-9,10(6*H*,9*bH*)-dione (4a)*: white solid; mp=255–257 °C; IR (KBr): 3476, 3238, 2927, 1723, 1608, 1547, 1494, 1451 cm⁻¹; ¹H NMR (400 MHz, DMSO-*d*₆), δ (ppm): 0.89 (3H, s), 0.96 (3H, s), 1.79 (1H, d, *J*=16.8 Hz), 1.89 (1H, d, *J*=15.6 Hz), 2.15 (1H, d, *J*=14.8 Hz), 2.41 (1H, d, *J*=17.2 Hz), 5.99 (1H, s), 6.59–6.60 (1H, m), 7.27–7.30 (3H, m), 7.45–7.57 (5H, m), 7.71–7.73 (1H, m).

*4b,9b-Dihydroxy-7,7-dimethyl-5-phenyl-4b,5,7,8-tetrahydroindeno[1,2-*b*]indole-9,10(6*H*,9*bH*)-dione (4b)*: white solid; mp=240–242 °C; IR (KBr): 3538, 3368, 2956, 1722, 1551, 1494, 1446 cm⁻¹; ¹H NMR (400 MHz, DMSO-*d*₆), δ (ppm): 0.87 (3H, s), 0.93 (3H, s), 1.78 (1H, d, *J*=17.2 Hz), 1.88 (1H, d, *J*=15.6 Hz), 2.12 (1H, d, *J*=15.6 Hz), 2.40 (1H, d, *J*=16.8 Hz), 6.03 (1H, s), 6.65 (1H, d, *J*=7.6 Hz), 7.30–7.33 (3H, m), 7.52–7.60 (4H, m), 7.70–7.71 (1H, d, *J*=7.2 Hz).

*4b,9b-Dihydroxy-7,7-dimethyl-5-phenyl-4b,5,7,8-tetrahydroindeno[1,2-*b*]indole-9,10(6*H*,9*bH*)-dione (4c)*: white solid; mp=160–162 °C; IR (KBr): 3325, 2956, 1727, 1630, 1551, 1491, 1448 cm⁻¹; ¹H NMR (400 MHz, DMSO-*d*₆), δ (ppm): 0.87 (3H, s), 0.93 (3H, s), 1.78 (1H, d, *J*=17.2 Hz), 1.88 (1H, d, *J*=15.6 Hz), 2.12 (1H, d, *J*=15.6 Hz), 2.40 (1H, d, *J*=16.8 Hz), 6.04 (1H, s), 6.66 (1H, d, *J*=7.2 Hz), 7.24 (2H, d, *J*=8 Hz), 7.34 (1H, s), 7.50–7.69 (5H, m).

*4b,9b-Dihydroxy-7,7-dimethyl-5-phenyl-4b,5,7,8-tetrahydroindeno[1,2-*b*]indole-9,10(6*H*,9*bH*)-dione (4d)*: pale yellow solid; mp=201–205 °C; IR (KBr): 3068, 3493, 3376, 2958, 1727, 1529, 1451 cm⁻¹; ¹H NMR (400 MHz, DMSO-*d*₆), δ (ppm): 0.88 (3H, s), 0.94 (3H, s), 1.81 (1H, d, *J*=17.2 Hz), 1.90 (1H, d, *J*=15.6 Hz), 2.15 (1H, d, *J*=16 Hz), 2.52 (1H, m), 6.14 (1H, s), 6.64–6.66 (1H, m), 7.53–7.78 (6H, m), 8.30–8.34 (2H, m).

*4b,9b-Dihydroxy-7,7-dimethyl-5-phenyl-4b,5,7,8-tetrahydroindeno[1,2-*b*]indole-9,10(6*H*,9*bH*)-dione (4e)*: yellow solid; mp=175–177 °C; IR (KBr): 3317, 2957, 1727, 1610, 1556, 1497 cm⁻¹; ¹H NMR (400 MHz, DMSO-*d*₆), δ (ppm): 0.90 (3H, s), 0.94 (3H, s), 1.85–1.93 (2H, m), 2.17 (1H, d, *J*=16 Hz), 2.57 (1H, d, *J*=17.2 Hz), 6.18 (1H, s), 6.67 (1H, d, *J*=6.8 Hz), 7.53–7.61 (5H, m), 7.70–7.72 (1H, m), 8.34

(2H, d, $J=8.8$ Hz). ¹³C NMR (100 MHz, DMSO-d₆): 26.0, 29.4, 33.7, 37.1, 51.1, 97.4, 107.7, 123.3, 124.4, 124.5, 129.0, 130.4, 134.5, 135.2, 142.9, 145.8, 146.8, 162.2, 189.9, 197.2. Anal. calcd. for C₂₃H₂₀N₂O₆: C 65.71, H 4.79, N 6.66%. Found: C 65.70, H 4.81, N 6.68%.

4b,9b-Dihydroxy-7,7-dimethyl-5-phenyl-4b,5,7,8-tetrahydroindenol[1,2-b]indole-9,10(6H,9bH)-dione (4f): white solid; mp=241–243 °C; IR (KBr): 3416, 2957, 1714, 1601, 1569, 1447 cm⁻¹; ¹H NMR (400 MHz, DMSO-d₆), δ (ppm): 0.84 (3H, s), 0.95 (3H, s), 1.92–2.05 (4H, m), 5.98 (1H, s), 6.65 (1H, m), 7.36 (1H, s), 7.36–7.54 (5H, m), 7.71 (1H, m), 7.81 (1H, d, $J=7.2$ Hz).

4b,9b-Dihydroxy-7,7-dimethyl-5-phenyl-4b,5,7,8-tetrahydroindenol[1,2-b]indole-9,10(6H,9bH)-dione (4g): yellow solid; mp=205–207 °C; IR (KBr): 3641, 3459, 3349, 3162, 2957, 1712, 1618, 1592, 1444 cm⁻¹; ¹H NMR (400 MHz, DMSO-d₆), δ (ppm): 0.83 (3H, s), 0.94 (3H, s), 1.85–1.95 (2H, m), 2.07 (1H, d, $J=16$ Hz), 2.15 (1H, d, $J=17.2$ Hz), 5.77 (1H, s), 6.67 (1H, d, $J=6.4$ Hz), 6.84 (1H, d, $J=7.6$ Hz), 6.92–7.01 (2H, m), 7.26 (1H, t, $J=7.2$ Hz), 7.49 (2H, m), 7.59 (1H, d, $J=7.2$ Hz), 7.66 (1H, d, $J=6.4$ Hz), 9.41 (1H, s). ¹³C NMR (100 MHz, DMSO-d₆): 27.4, 28.7, 33.1, 36.3, 51.3, 83.2, 95.9, 104.0, 115.7, 118.9, 122.6, 122.7, 124.6, 129.6, 131.2, 134.6, 148.0, 154.2, 165.0, 188.8, 198. Anal. calcd. for C₂₃H₂₀N₂O₆: C 70.58, H 5.41, N 3.58%. Found: C 70.57, H 5.44, N 3.56%.

4b,9b-Dihydroxy-7,7-dimethyl-5-phenyl-4b,5,7,8-tetrahydroindenol[1,2-b]indole-9,10(6H,9bH)-dione (4h): brown solid; mp=258–260 °C; IR (KBr): 3321, 2927, 1721, 1603, 1552, 1455 cm⁻¹; ¹H NMR (400 MHz, DMSO-d₆), δ (ppm): 0.85 (3H, s), 0.93 (3H, s), 1.78 (1H, d, $J=16.8$ Hz), 1.87 (1H, d, $J=15.6$ Hz), 2.09 (1H, d, $J=16$ Hz), 2.26 (1H, d, $J=17.2$ Hz), 5.88 (1H, s), 6.71 (1H, d, $J=7.6$ Hz), 6.82 (2H, d, $J=8.4$ Hz), 7.02–7.08 (3H, m), 7.52 (1H, d, $J=7.2$ Hz), 7.57 (1H, d, $J=7.2$ Hz), 7.69 (1H, d, $J=7.6$ Hz), 9.77 (1H, s). ¹³C NMR (100 MHz, DMSO-d₆): 26.6, 29.2, 33.2, 36.8, 51.1, 83.2, 96.3, 104.5, 115.3, 123.0, 125.1, 126.6, 130.0, 134.6, 134.7, 147.2, 157.1, 163.9, 188.8, 197.6. Anal. calcd. for C₂₃H₂₀N₂O₆: C 70.58, H 5.41, N 3.58%. Found: C 70.57, H 5.43, N 3.60%.

4b,9b-Dihydroxy-7,7-dimethyl-5-phenyl-4b,5,7,8-tetrahydroindenol[1,2-b]indole-9,10(6H,9bH)-dione (4i): white solid; mp=235–238 °C; IR (KBr): 3465, 3241, 2947, 1724, 1605, 1548 cm⁻¹; ¹H NMR (400 MHz, DMSO-d₆), δ (ppm): 1.77–1.79 (2H, m), 1.94–1.98 (1H, m), 2.10–2.14 (2H, m), 2.38–2.42 (1H, m), 5.96 (1H, s), 6.60 (1H, d, $J=6.8$ Hz), 7.21 (1H, s), 7.3 (2H, d, $J=6$ Hz), 7.46–7.52 (5H, m), 7.70 (1H, d, $J=7.2$ Hz).

4b,9b-Dihydroxy-7,7-dimethyl-5-phenyl-4b,5,7,8-tetrahydroindenol[1,2-b]indole-9,10(6H,9bH)-dione (4j): white solid; mp=205–208 °C; IR (KBr): 3462, 3180, 1729, 1602, 1550 cm⁻¹; ¹H NMR (400 MHz, DMSO-d₆), δ (ppm): 1.78 (2H, m), 2.01 (3H, m), 2.40 (1H, m), 6.01 (1H, s), 6.66 (1H, d, $J=7.2$ Hz), 7.29 (1H, s), 7.33 (2H, d, $J=8$ Hz), 7.55 (3H, m), 7.70 (1H, d, $J=6.8$ Hz).

4b,9b-Dihydroxy-7,7-dimethyl-5-phenyl-4b,5,7,8-tetrahydroindenol[1,2-b]indole-9,10(6H,9bH)-dione (4k): white solid; mp=202–204 °C; IR (KBr): 3190, 1730, 1598, 1546, 1491 cm⁻¹; ¹H NMR (400 MHz, DMSO-d₆), δ (ppm): 1.78 (2H, m), 1.96–2.00 (1H, m), 2.10 (2H, m), 2.37–2.44 (1H, m), 6.00 (1H, s), 6.66 (1H, d, $J=7.2$ Hz), 7.26 (3H, m), 7.52–7.71 (5H, m).

*4b,9b-Dihydroxy-7,7-dimethyl-5-phenyl-4b,5,7,8-tetrahydroindeno[1,2-*b*]indole-9,10(6*H*,9*bH*)-dione (4l)*: white solid; mp=234–236 °C; IR (KBr): 3170, 2927, 1724, 1559, 1509, 1462 cm⁻¹; ¹H NMR (400 MHz, DMSO-*d*₆), δ (ppm): 1.76 (2H, m), 1.93–2.10 (3H, m), 2.37 (4H, s), 5.91 (1H, s), 6.65 (1H, d, *J*=7.2 Hz), 7.13 (1H, s), 7.17 (2H, d, *J*=7.6 Hz), 7.27 (2H, d, *J*=8 Hz), 7.51–7.57 (2H, m), 7.70 (1H, d, *J*=7.2 Hz).

*4b,9b-Dihydroxy-7,7-dimethyl-5-phenyl-4b,5,7,8-tetrahydroindeno[1,2-*b*]indole-9,10(6*H*,9*bH*)-dione (4m)*: yellow solid; mp=195–197 °C; IR (KBr): 3345, 2946, 1719, 1614, 1550, 1511 cm⁻¹; ¹H NMR (400 MHz, DMSO-*d*₆), δ (ppm): 1.76 (2H, m), 1.92–1.97 (1H, m), 2.08 (2H, m), 2.30–2.34 (1H, m), 3.79 (3H, s), 5.91 (1H, s), 6.68 (1H, d, *J*=7.2 Hz), 7.01 (2H, d, *J*=8 Hz), 7.11 (1H, s), 7.19 (2H, d, *J*=7.2 Hz), 7.51–7.57 (1H, m), 7.70 (2H, d, *J*=6.8 Hz).

*4b,9b-Dihydroxy-7,7-dimethyl-5-phenyl-4b,5,7,8-tetrahydroindeno[1,2-*b*]indole-9,10(6*H*,9*bH*)-dione (4n)*: white solid; mp=234–236 °C; IR (KBr): 3160, 2928, 1724, 1545, 1469 cm⁻¹; ¹H NMR (400 MHz, DMSO-*d*₆), δ (ppm): 1.10 (3H, s), 1.71–1.78 (2H, m), 1.93–1.98 (2H, m), 2.11–2.14 (2H, m), 2.32 (3H, s), 5.85 (1H, s), 6.65 (1H, m), 7.03 (1H, s), 7.16–7.21 (2H, m), 7.50–7.55 (3H, m), 7.72 (1H, m).

Results and discussion

Characterization of magnetic MMT@Fe₃O₄-NPs

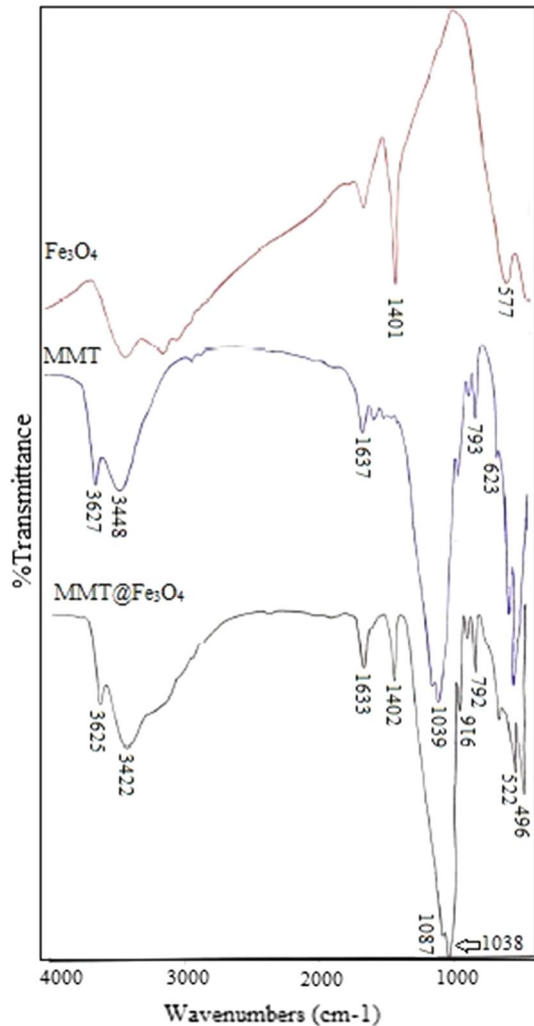
The magnetically heterogeneous organocatalyst, MMT@Fe₃O₄-NPs, was characterized by XRD, SEM, EDX, VSM and FT-IR spectroscopy.

The FT-IR spectra of Fe₃O₄, MMT, and MMT@Fe₃O₄ are shown in Fig. 1. The band around 916 cm⁻¹ was attributed to Al–Al–OH due to of the large rate of Al in the octahedral site of oxygen. The band at 522 cm⁻¹ was assigned to Si–O–Al. Hydroxyl stretching vibration of structural MMT was discovered at 3422 cm⁻¹. The Fe–O stretching vibration bond was observed at 577 cm⁻¹. The bending modes of Al–Mg–OH and Si–O–Fe are found at 845 and 469 cm⁻¹, respectively. The band at 1402 cm⁻¹ can be assigned to N–H in the MMT-Fe₃O₄ structure. All three FT-IR spectra confirm the presence of Fe₃O₄-NPs on the MMT. Thus, the magnetic nanocomposite (NC) is stable during the synthesis of indeno[1,2-*b*]indole derivatives in aqueous media.

The XRD patterns of MMT@Fe₃O₄ are displayed in Fig. 2. All of the characteristic peaks of magnetic Fe₃O₄-NPs are existent in the diffraction pattern and the diffraction peaks match with the standard XRD pattern (JCPDS file no. 75-0449), relevant to the crystalline structure with a spinel structure. The well-defined peaks are shown at 5.8°, 17.7°, 19.8°, 29.5°, 34.9°, 36.0°, 54.0° and 61.9° related to the hexagonal structure of MMT. According to XRD pattern, 2 θ =20.8° and 26.6° display quartz in MMT.

As illustrated in Fig. 3, the SEM image specified the microstructures and morphologies of the sample. The obtained SEM images of NPs intelligibly showed that Fe₃O₄-NPs were properly composed with the surface of MMT. Thus,

Fig. 1 FT-IR spectra of Fe₃O₄, MMT, and MMT@Fe₃O₄



MMT@Fe₃O₄ composite was successfully synthesized according to these results. The EDX image in Fig. 4 identifies the elemental oxygen and iron in Fe₃O₄-NPs, and carbon, sodium, silicon, aluminum and magnesium in MMT. So, the presence of elemental compounds in the MMT and Fe₃O₄-NPs without any impurity peaks is clearly seen in this spectrum. Figure 5 presents the VSM results to examine the magnetic properties of MMT@Fe₃O₄ NCs and Fe₃O₄ being trapped in the MMT layers. TGA of the MMT@Fe₃O₄ NC is shown in Fig. 6. The weight loss below 200 °C could be assigned the evaporation of adsorbed water. The weight loss observed at 200–400 °C in the TGA curve is mainly related to the desorption of crystal water. The final mass loss at temperatures ranging from 550 to 750 °C confirmed the loss of structural hydroxyl groups.

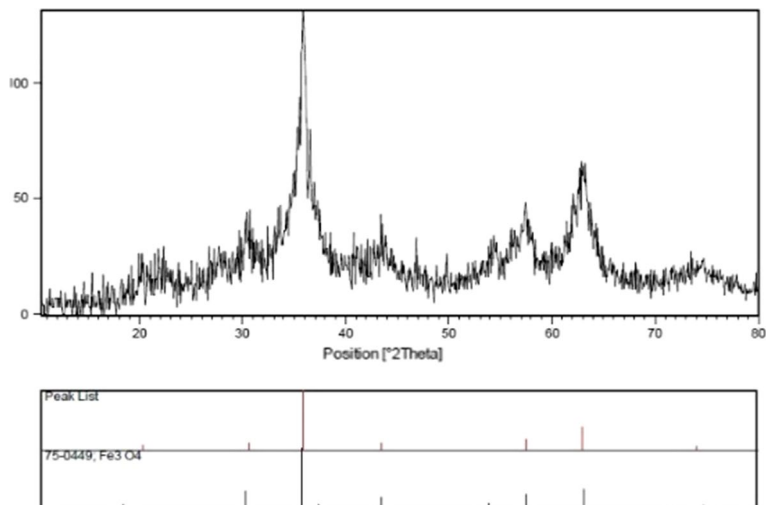
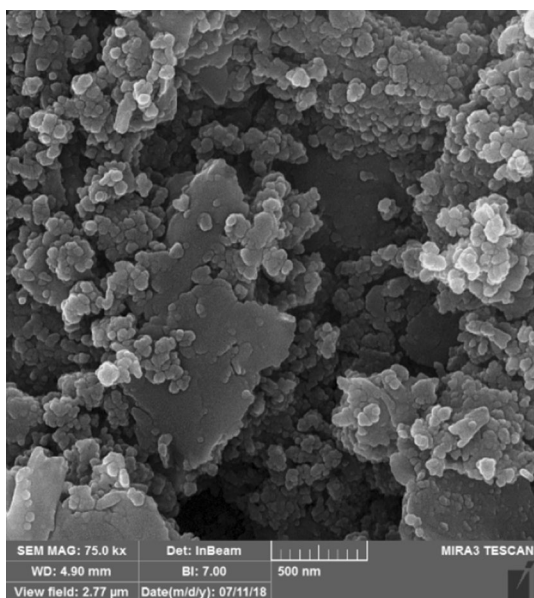


Fig. 2 The X-ray diffraction patterns of MMT@Fe₃O₄

Fig. 3 The SEM image of MMT@Fe₃O₄



Investigation of catalyst activity

At first, we selected a model reaction containing ninhydrin, dimedone and aniline in the presence of MMT@Fe₃O₄ as a magnetic NC. Some previous work for the formation of indeno[1,2-*b*]indole derivatives was performed to compare the influence of MMT@Fe₃O₄ against reported catalyst in the literature. The outcomes are shown in Table 1. MMT@Fe₃O₄ was recognized to be an efficient catalyst because

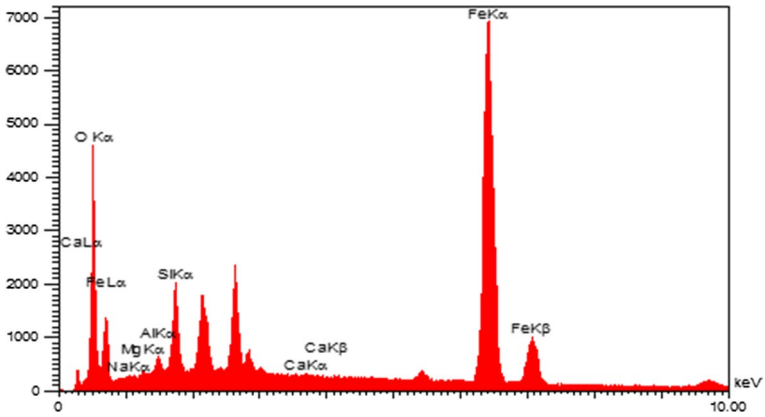


Fig. 4 EDX spectrum of MMT@Fe₃O₄

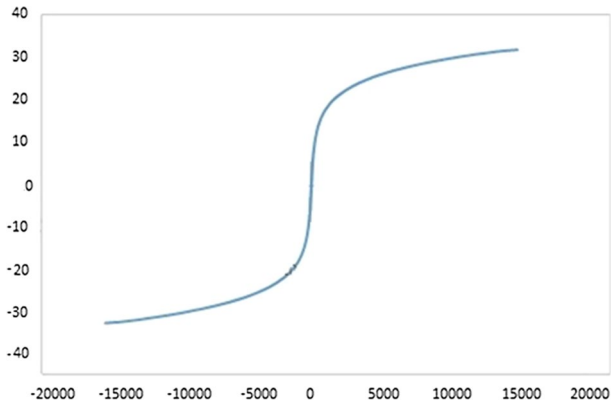


Fig. 5 The VSM curve of MMT@Fe₃O₄

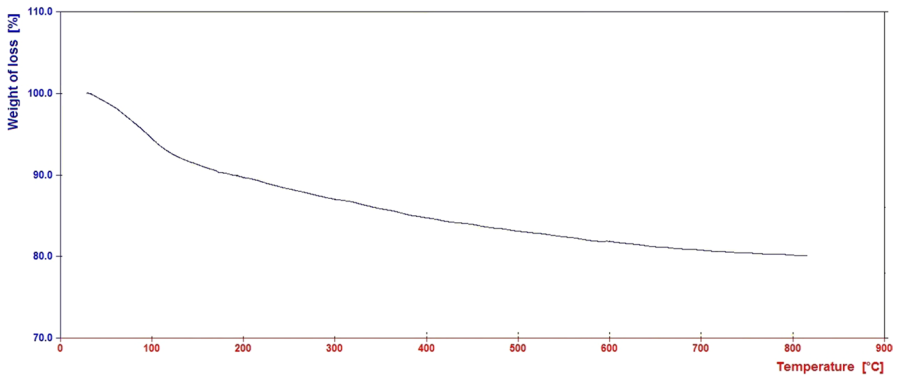


Fig. 6 The TGA curve of MMT@Fe₃O₄

Table 1 Comparison of results for the synthesis of indeno[1,2-*b*]indoles with various catalysts

Entry	Catalyst	Time	Yield (%) ^a /Ref
1	SnO ₂ QDs	2.5 h	89/[18]
2	C@TiO ₂ -SO ₃ H-IL1	1 h	92/[19]
3	MMT@Fe ₃ O ₄	20 min	97/This work

^aIsolated yield

it improved the reaction time and yield. To investigate the optimal amount of the catalyst, the reaction was done in the presence of different amounts of NC (Table 2). As shown in Table 2, the best amount of the catalyst was 0.02 g and in the absence of a magnetic catalyst, no product was gained. Our studies demonstrated MMT@Fe₃O₄ has supreme catalytic activity for the synthesis of indeno[1,2-*b*]indolines compared to another catalyst. This is because MMT@Fe₃O₄ containing MMT has active magnetite sites. Accordingly, MMT@Fe₃O₄ was chosen for this synthesis because it is obvious its catalytic system speeds up the reaction. Thereafter, the reaction was tested in different solvents such as H₂O, EtOH, H₂O/EtOH, CH₃CN, dimethylformamide (DMF) and toluene. The results are summarized in Table 3. It is clear that polar solvents versus non-polar solvents gave more yields. Among the polar solvents, water had the best effect. After that, we performed the model reaction at different temperatures (r.t., 50, 60, 70, 100 °C) in water. The results are summarized in Table 4. As shown in Table 4, one of the important factors in the speed and efficiency of the reaction is the effect of the reaction temperature. The best temperature for this reaction was 70 °C; below this temperature, there was not much product and no significant changes in the reaction efficiency were observed at the reflux temperature.

In continuation of our research, after the optimization of all the reaction parameters, a series of different amines with the electron-donating and electron-withdrawing groups were used to investigate these three-component reactions under MMT@Fe₃O₄ catalysis. It is absolutely clear that using aromatic amine derivatives with the electron-donating group such as OH, CH₃ and OCH₃ reacted better than aromatic amine derivatives with an electron-withdrawing group and unsubstituted aromatic amine (Table 5).

Table 2 Optimization amount of MMT@Fe₃O₄ catalyst

Entry	Amount of catalyst (g)	Time	Yield (%) ^a
1	0	24 h	Trace
2	0.005	3 h	56
3	0.01	1.5 h	80
4	0.02	30 min	92
5	0.03	45 min	90

Reaction conditions: aniline (1 mmol), dimedone (1 mmol), ninhydrin, 5 ml of H₂O^aIsolated yield

Table 3 The effect of different solvents in the synthesis of 4a

Entry	Solvent	Time (min)	Yield (%) ^a
1	H ₂ O	30	92
2	EtOH	70	35
3	H ₂ O/EtOH(1:1)	60	40
4	CH ₃ CN	65	50
5	DMF	80	20
6	Toluene	80	28

Reaction conditions: aniline (1 mmol), dimedone (1 mmol), ninhydrin, MMT@Fe₃O₄ (0.02 g)

^aIsolated yield of the pure compound

Table 4 Effect of temperature on the yield of reaction

Entry	Temperature	Time (min)	Yield (%) ^a
1	r.t	240	25
2	50	180	45
3	60	90	82
4	70	30	92
5	100	45	90

Reaction conditions: aniline (1 mmol), dimedone (1 mmol), ninhydrin, MMT@Fe₃O₄ (0.02 g), water (5 ml)

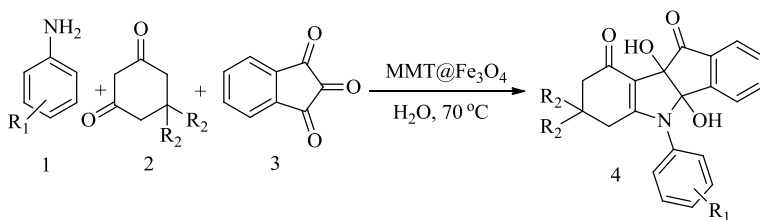
^aIsolated yield of the pure compound

Reusability test of magnetic catalyst

A very important factor of magnetic heterogeneous NC is its level of reusability and ease of recovery. To illuminate this issue, the reaction was carried out under identical conditions in the presence of a reusable catalyst. After completion of the reaction, the catalytic system was separated from the reaction mixture by an external magnet, washed with water several times, air-dried and reused directly with fresh substrates under similar conditions without considerable loss of catalytic activity (Fig. 7).

The proposed reaction mechanism

The probable mechanism for the formation of indeno[1,2-*b*]indolines is indicated in Scheme 2. At the outset, the reaction likely proceeds via MMT@Fe₃O₄ catalyzing the condensation of 1,3-diketo compound and amine to form intermediate I (enaminone). Fe₃O₄-NPs, as powerful Lewis acids, promoted the condensation between 1,3-diketo compound and amine derivatives, by enhancing the electrophilicity of carbonyl groups. In the next step, MMT@Fe₃O₄ helped the reaction between intermediate I and ninhydrin by Michael addition to form intermediate II. In the final step, intramolecular electrophilic cyclization generated

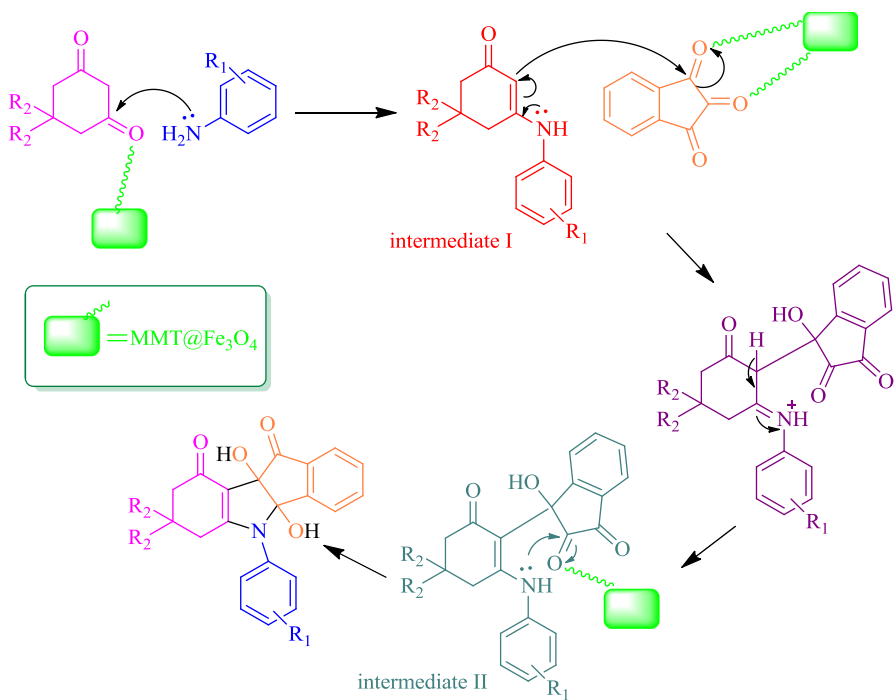
Table 5 Synthesis of indeno[1,2-*b*]indole derivatives 4^a

Entry	R ₁	R ₂	Product	Time (min)	Yield (%) ^b	Melting point (°C)	Melting point (°C) [Ref.]
1	H	CH ₃	4a	30	92	255–257	210–212 [18]
2	4-Cl	CH ₃	4b	35	90	240–242	238–240 [18]
3	4-Br	CH ₃	4c	35	90	160–162	160–162 [18]
4	3-NO ₂	CH ₃	4d	35	89	201–205	170–172 [18]
5	4-NO ₂	CH ₃	4e	40	90	175–177	New
6	2-Cl	CH ₃	4f	30	87	241–243	230–231 [19]
7	2-OH	CH ₃	4g	35	92	205–207	New
8	4-OH	CH ₃	4h	20	94	258–260	New
9	H	H	4i	30	92	235–238	218–220 [18]
10	4-Cl	H	4j	35	91	198–200	170–172 [21]
11	4-Br	H	4k	35	90	202–204	200 [21]
12	4-CH ₃	H	4l	20	96	234–236	228–231 [22]
13	4-OCH ₃	H	4m	20	97	195–197	194–196 [18]
14	2,4-(CH ₃) ₂	H	4n	20	97	234–236	230–233 [21]

^aaniline (1 mmol), 1,3-diketone compound (1 mmol), ninhydrin (1 mmol), MMT@Fe₃O₄ (0.02 g), water (5 ml)

^bIsolated yield of the pure compound

**Fig. 7** Reusability results of nanocatalyst in the model reaction (4a)



Scheme 2 Proposed reaction mechanism for the synthesis of indeno[1,2-*b*]indoline derivatives

five-membered rings, which was a result of reaction between MMT@Fe₃O₄ and intermediate II.

Conclusion

In this paper, magnetic organocatalyst (MMT@Fe₃O₄) as a heterogeneous, easy-to-prepare, reusable, low-cost and nontoxic catalyst was utilized for the synthesis of indeno[1,2-*b*]indole derivatives. This novel procedure provides many advantages, including the use of a green solvent (H₂O), being a simple and environmentally benign method, easy isolation, shorter reaction time and higher yield than available methods. The development of green chemistry methods using this catalytic system is a promising and expedient approach.

Acknowledgements The authors gratefully acknowledge the financial support from the University of Kashan for supporting this work by Grant No. 363022/12.

References

1. C. Bal, B. Baldeyrou, F. Moz, A. Lansiaux, P. Colson, L. Kraus- Berthier, S. L'éonce, A. Pierré, M.-F. Boussard, A. Rousseau, M. Wierzbicki, C. Bailly, *Biochem. Pharmacol.* **68**, 1911 (2004)
2. D.W. Brown, P.R. Graupner, M. Sainsbury, H.G. Shertzer, *Tetrahedron* **47**, 4383 (1991)
3. H. J. Hemmerling, C. Götz and J. Jose Annual Meeting of the German Pharmaceutical Society (DPhG), Marburg 2006, Poster P32 (b) H. J. Hemmerling, C. Götz and J. Jose *J.EP* 2007/008624, 2007; WO 2008040547, 2008
4. J.A. Butera, S.A. Antane, B. Hirth, J.R. Lennox, J.H. Sheldon, N.W. Norton, D. Warga, T.M. Argenterii, *Bioorg. Med. Chem. Lett.* **11**, 2093 (2001)
5. C. P. Miller, M. D. Collini and B. D. Tran *US* 6107292, 2000
6. M. Ruzzene, L. Pinna, *Biochem. Biophys. Acta Proteins Proteomics* **1804**, 499 (2010)
7. K. Ahmed, G. Wang, G. Unger, J. Slaton, K. Ahmed *Adv. Enzyme Regul.* **48**, 179 (2008)
8. N.D. Cuong, T.T. Hoa, D.Q. Khieu, T.D. Lam, N.D. Hoa, N.V. Hieu, *J. Alloys Compd.* **523**, 120 (2012)
9. G. Mihoc, R. Ianos, C. Păcurariu, I. Lazău, *J. Therm. Anal. Calorim.* **112**, 391 (2013)
10. M. Abbas, B. Parvatheeswara Rao, S.M. Naga, M. Takahashi, C. Kim, *Ceramics Int.* **39**, 7605 (2013)
11. B.M. Choudary, N.S. Chowdari, M.L. Kantam, *Tetrahedron* **56**, 7291 (2000)
12. G.B.B. Varadwaj, K.M. Parida, *RSC Adv.* **3**, 13583 (2013)
13. B.S. Kumar, A. Dhakshinamoorthy, K. Pitchumani, *Catal. Sci. Technol.* **4**, 2378 (2014)
14. S. Ahmadi, C.H. Chia, S. Zakaria, K. Saeedfar, N. Asim, *J. Magn. Magn. Mater.* **324**, 4147 (2012)
15. K. Raja, S. Verma, S. Karmakar, S. Kar, S.J. Das, K.S. Bartwal, *Cryst. Res. Technol.* **46**, 497 (2011)
16. G. Gao, R. Shi, W. Qin et al., *J. Mater. Sci.* **45**, 3483 (2010)
17. N. Wang, L. Zhu, D. Wang, M. Wang, Z. Lin, H. Tang, *Ultrason. Sonochem.* **17**, 526 (2010)
18. K. Pradhan, S. Paul, A.R. Das, *RSC Adv.* **5**, 12062 (2015)
19. M. Kour, M. Bhardwaj, H. Sharma, S. Paul, H.C. James, *New J. Chem.* **41**, 5521 (2017)
20. X. Zheng, J. Dou, J. Yuan, W. Qin, X. Hong, A. Ding, *J. Environ. Sci.* **56**, 12 (2017)
21. G. Lobo, M. Monasterios, J. Rodrigues, N. Gamboa, M.V. Capparelli, J. Martínez-Cuevas, M. Lein, K. Jung, C. Abramjuk, J. Charris, *Eur. J. Med. Chem.* **96**, 281 (2015)
22. X. Chen, Y. Liu, X. Chen, Y. Liu, *Heterocycl. Commun.* **22**, 161 (2016)